Hindawi
Modelling and Simulation in Engineering
Volume 2019, Article ID 1024365, 15 pages
https://doi.org/10.1155/2019/1024365

Research Article

Mathematical Modeling of Multiple Quality Characteristics of a Laser Microdrilling Process Used in Al7075/SiC$_p$ Metal Matrix Composite Using Genetic Programming

Mohammed Yunus and Mohammad S. Alsoufi

Department of Mechanical Engineering, College of Engineering and Islamic Architecture, Umm Al-Qura University, Al-Abdiah, Makkah 24231, Saudi Arabia

Correspondence should be addressed to Mohammed Yunus; yunus.mohammed@rediffmail.com

Received 16 August 2018; Accepted 12 November 2018; Published 2 January 2019

Academic Editor: Aiguo Song

The conventional method for machining metal matrix composites (MMCs) is difficult on account of their excellent characteristics compared with those of their source materials. Modern laser machining technology is a suitable noncontact method for machining operations of advanced engineering materials due to its novel advantages such as higher productivity, ease of adaptation to automation, minimum heat affected zone (HAZ), green manufacturing, decreased processing costs, improved quality, reduced wastage, removal of finishing operations, and so on. Their application includes hole drilling in an aircraft engine components such as combustion chambers, nozzle guide vanes, and turbine blades made up of MMCs which meet quality standards that determine their suitability for service use. This paper presents a derived mathematical model based on evolutionary computation methods using multivariate regression fitting for the prediction of multiple characteristics (circularity, taper, spatter, and HAZ) of neodymium: yttrium aluminum garnet laser drilling of aluminum matrix/silicon carbide particulate (Al/SiCp) MMCs using genetic programming. Laser drilling input factors such as laser power, pulse frequency, gas pressure, and pulse width are utilized. From a training dataset, different genetic models for multiple quality characteristics were obtained with great accuracy during simulated evolution to provide a more accurate prediction compared to empirical correlations.

1. Introduction

Metal matrix composites (MMCs) are substances which blend a tough metallic matrix with a hard ceramic reinforcement possessing excellent features such as high strength to wear ratio, high modulus, and wear and corrosion resistance [1]. MMCs are broadly used in the fields of the aerospace, automotive, electronics, and metallic industries. MMCs comprise a metal as a base material (matrix) and hard ceramic particles such as B_4C, SiC, and Al_2O_3 as reinforcement (long fibers, short whiskers, or particulates in irregular or spherical shapes). The properties of MMCs are judged by matrix, reinforcement, and interface between them [2]. They are a material which is difficult to machine due to the presence of hard ceramic particles [3]. Most of the research in the machining of Al/SiCp MMCs has focused on turning and milling, whereas drilling has been given less attention.

1.1. Laser Drilling. The laser drilling system is growing exponentially to suit the alternative program for achieving the major demands of aerospace, automobile, metallic, and electric industrial potential, especially microhole drilling in different components such as watches and turbine blades, fuselages, printed circuit boards, and so on [3]. Pulsed Nd: YAG laser microhole drilling has gained popularity in recent years to be used as an indispensable tool for microhole drilling of components for technologically advanced industries. Laser microhole drilling processes are successfully employed to both conductive and nonconductive materials to remove by evaporation, and the amount of molten material removed depends on the penetration of laser energy generated from a sequence of laser pulses at the same place [4]. Laser drilling in the production industry has been associated with the various advantages of a high rate of machining, noncontact method; hence, there is no damage to tool or tool wear, increased product quality, and less wastage. Highly reflective materials require a low amount of laser power with a short wavelength of Nd:YAG (compared with CO_2 lasers) [5]. While it possesses several advantages and is widely approved by advanced industries, it also has some defects such as taperness, noncircular holes, HAZ, recast layer, and so on [6].

1.2. Genetic Programming. Genetic programming (GP) is the most effective tool used to predict the behaviour of various processes and for the formation of empirical modeling. Normally, GP supports the process of evolution in nature—Darwin's theory of "*survival of the fittest*"—to find the best solution to an assigned problem. GP is known as the generalized form of the genetic algorithm (GA) and has been extensively studied [7–9]. In GP, the model is represented by terminals and functions. A well-known implementation of GP is in symbolic regression and is used to determine the mathematical expression for a given set of variables and functions. The function is generated using a Boolean operator (AND, OR, NOT, or AND NOT), nonlinear operators (sin, cos, tan, exp, tanh, and log), and from basic mathematical operators (+, −, /, and ×). The fitness function is calculated as the error between the actual value and the predicted value of the symbolic expressions. In GP, individual terms are randomly initialized, and the population is progressed to find out the optimal solutions through various operations such as reproduction, crossover, and mutation. The reproduction process produces children as an input to the next generation by replicating a fraction of the parent selected by the current generation. Individuals having highest fitness values in the population are selected as the parent and used for reproduction. Normally, the crossover operation produces children by exchanging some parts of their selected parents. The crossover operation is divided into two types (subtree and node crossover). However, the subtree crossover has shown more significant effect than the node crossover.

A variety of methods are available to develop relationships between inputs and outputs for evaluating outputs under varying input conditions without experimental work. These forecasting output data are derived in the form of equations using artificial neural network, statistical regression methods like linear regression, response surface, ANOVA, etc., with limited accuracy. To obtain higher accuracy at about 99.3 to 99.8% for the mathematical model derived, the effective method available is genetic programming which is an application of machine learning or artificial intelligence using inbuilt algorithms. The use of the GP approach with experimental data to develop a mathematical model involving laser microhole drilling input and output parameters is presented in this work. These mathematical models can be used to study the production of high-quality microdrills of the pulsed Nd:YAG laser used in Al7075/SiCp MMCs by minimizing the microhole drilling defects, such as the degree of taperness of a hole, spatter, and heat affected zone width, and to maximize a hole circularity [10]. The various drilling input parameters involved are pulse power (v_0), pulse frequency (v_1), assistance of gas pressure (v_2), and pulse width (v_3) [11].

2. Materials and Methods

In the present work, using the stir casting technique, an MMC consisting of aluminum alloy 7075 as a base metal reinforced with particulates of silicon carbide having a size of 40–50 μm for 10% volume fractions is produced. The microholes were drilled onto MMC plates using the pulsed Nd:YAG laser beam system (Model: JK300D), and the tests were carried out at its maximum power capacity of 16 kW. Various input parameters such as laser input power (v_0), pulse frequency (v_1), assistance of gas pressure (v_2), and pulse width (v_3) at different levels have been selected. The experimental results for various levels of input factors of laser microhole drilling of MMC (Al7075/10%SiCp) plate of 2 mm thick are shown in Tables 2–5. For a smaller diameter hole, laser microdrilling is preferred, especially when the materials are very hard, extra thin, or made of glass and composites. The quality of these holes mainly depends on heat affected zone (HAZ) of hole walls, taperness formed when the hole is enlarged, circularity to maintain the uniform dimension of the circular hole, and spatter occurring at the ends of a hole during resolidification of material [12, 13].

The input parameters of different levels can improve the quality of drilled holes. The quality of holes was determined using optical measuring microscope OLYMPUS STM6 on a cut sectioned hole sample by measuring circularity, spatter, HAZ, and taper characteristics, and in each experimental run, the laser was drilled at a spot size of 180 μm [10]. Various studies have been conducted to investigate the effects of input control parameters on the defects developed by the laser microdrilling process [14, 15]. Due to an internal focusing of the issue of a laser drilling process, hole taperness and noncircularity affect the quality of holes [16]. Normally, there is spatter accumulation due to an incomplete suspension of removed MMC at the drilling zone which resolidifies and adheres around the whole circumference. Hence, it is advisable to produce high-quality circular microdrilled holes with the minimum amount of taper, spatter, and HAZ width. The above-said qualities are to be determined by the level of input parameters which requires a mathematical model to study the process condition capable of producing the desired quality of product. However, this model is to be derived in such a way that all the characteristics measuring qualities are quickly measurable simultaneously [11].

3. Genetic Programming Methodology

Various stages of GP involved in the flowchart are as follows:

For the analysis of multiple characteristics of neodymium: yttrium aluminum garnet laser drilling of aluminum matrix/silicon carbide particulate MMCs such as circularity, taper, spatter, and HAZ, data accumulations of experiments were carried out as per stages involved in Figure 1. The accumulated data were randomized using notitia Discipulus^{TM} software and were provided to the

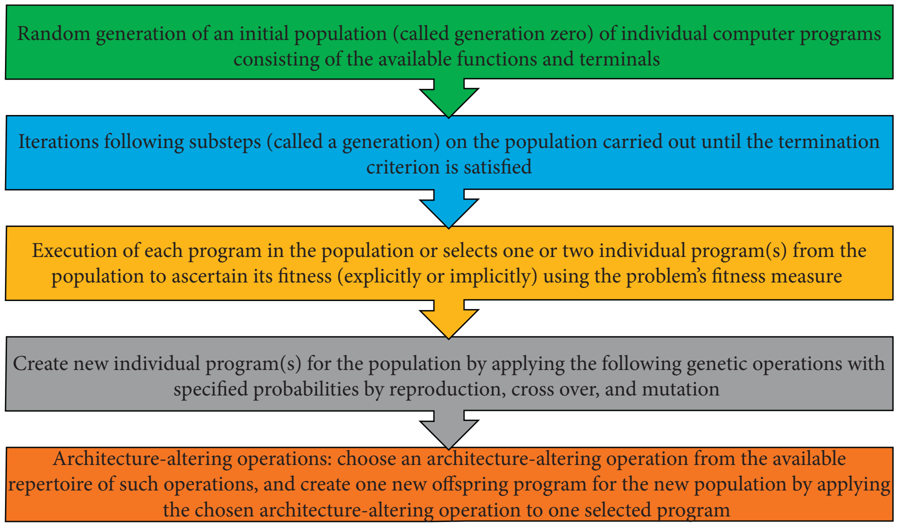

Figure 1: Stages involved in genetic programming.

software in three groups, viz., training, validation, and applied [17]. The three sets of data are generated by experimental results provided. Higher numbers of experiment running around more than 100 are required for best solution. Test runs were conducted to determine desirable parameters generating an optimal solution in the minimum possible time. Initially, the tests were carried out at the default parameter settings, such as population size, crossover rate, DSS subset size, and so on, and later varied to find optimum values [18]. The different parameters involved in achieving the final mathematical model satisfying the results are tabulated in Table 1. It shows the flow of set required to achieve the final model which could provide us a mathematical model satisfying the above conditions of the quantity involved [19].

Table 1: Parameter setting for genetic programming.

Parameters	Value assigned
Population size (P)	500
Number of generations	1000
Maximum depth of tree	6
Maximum generation	50
Functional set	Multiply, plus, minus, divide
Terminal set	(v1, v2, v3, v4, v5, v6, −10, 10)
Number of runs	110
Mutation rate	0.10
Crossover rate	75% nonhomologous 25% homologous
Reproduction rate	0.05
Fitness, r^2	The square root of the sum of the square of absolute value of the differences (errors), between the program's output and the observed data.
Termination	An individual emerges whose sum of absolute errors is less than specified: (a) required number of runs be completed or (b) required correlation coefficient is obtained
Terminal set	T = {P, random-constants}

3.1. Regression and Fitness Measurement. Regression analysis is a stochastic method in which symbolic regression finds both the working model of output (or target) function and its inputs (or fixed coefficients), or at least an approximation (error measurement fit by linear or square). Fitness measurement indicates how far the output value predicted by the GP concurs with the experimental value.

3.2. Correlation Coefficient, r/R. The linear correlation coefficient refers to measuring the strength and direction of a linear relationship held between two variables (output, M, and input, N), where r value lies such that $-1 < r < +1$ [8]. The signs indicate a strong positive linear correlation between M and N or perfect fit if r is close to +1 with an increase of M values; N values also increase, whereas r is close to −1 if M and N have a strong negative linear correlation such that with an increase of M values, N values decrease. For $r = 0$, there is no linear/weak correlation, and a value approaching zero represents a random, nonlinear relationship between the M and N. The square of the correlation coefficient provides you with the coefficient of determination, r^2, to find the proportion of the variance of output that is predictable from the inputs. This helps us to determine how certain one can be in making predictions from a defined model. r^2 defined from the ratio of the illustrated variation to the total variation in the range of $0 < r^2 < 1$ signifies the strength of the linear correlation between P and Q or represents the percentage of the data which is closest to the line of best fit [20]. If $r = 0.977$, then $r^2 = 0.994$, which means that 99.4% of the total variation in Q can be explained by the linear relationship between P and Q and the remaining 0.6% of the variation in Q continues unexplained [21].

3.3. Factors Involved in GP Modeling. The various parameters involved in modeling GP are tabulated in Table 1. It shows the flow of set required to achieve the final model which could provide you with a mathematical model satisfying the above conditions of the quantity involved.

4. Results and Discussion

The selection of precise instructions from set F and available terminal genes from set $f(0)$ play a vital role in GP modeling, and evolutionary process will build a mathematical model (i.e., organism) such that it is as fit as for the prediction of results. The model consists of both instructions and function genes behaving similarly to the character of computer programs differing in appearance and dimensions [20, 22]. Previously, extensive work on developing mathematical models was also carried out using linear regression, second order, and higher order equations using response surface methods, ANOVA, box, artificial neural network, and fuzzy logic method where the models of these methods develop the amount of error is very high compared to experimental values upto 3 digit numbers [24]. These analyses require high value of digit numbers not lower and decimal numbers for output values compared to values of inputs to accomplish accuracy. These methods are suitable for small number of inputs; otherwise, erroneous empirical relation would be generated. The above nonGP methods may use limited data according design matrix and orthogonal array of tables, and the equation will be developed by using optimal input values [24].

Using Grey–Taguchi method, the overall performance characteristic in Nd:YAG laser microdrilling of alumina was calculated using grey relational grade (GRG) to find a optimal parameter set for getting highest GRG. The optimal value of GRG was 0.9172 which indicates the effectiveness of the proposed approach and the highest value of GRG of 0.8989 for confirmation experiment. The overall quality feature is improved by 2.03% at optimal condition with HAZ width by 8.78%, and the hole taper worsened by 2.14%. This shows that, in multilevel optimization of performance, characteristics cannot reach simultaneously optimum value, instead they have to compromise between various performance characteristics to accomplish the optimum value pertaining to overall performance. Both the performance characteristics improve at optimum level with GRG of 0.1521 (19.88%). The taperness (from 0.0491 to 0.0476 rad) and HAZ width (from 0.2180 to 0.1683 mm) are decreased at the same time. From the results, we can see that optimum results can provide correlations at the accuracy level of 85% if outputs are limited to two numbers. By increasing output quality characteristics as well as input parameters and number of experiments, it is very difficult to arrive at optimal set and corresponding correlations obtained by regression analysis. Therefore GP-based solutions maintain an accuracy level beyond statistical analysis irrespective of number of outputs and inputs [25].

The model used experimental measurements collected by converting into three independent datasets such as training, validation, and applied. Independent input variables used are pulse power (v_0), pulse frequency (v_1), assistance of gas pressure (v_2), and pulse width (v_3) and circularity, spatter, heat affected zone, and taper as the dependent output variable. Various models for outputs are developed by GP using the training dataset [23]. Best mathematical models obtained from GP simulation are given by equations (1)–(4)

$$\text{circularity} = \frac{2GF^2 - v0}{v0} - \frac{1.745}{v0} + 0.904515, \tag{1}$$

$$\text{spatter} = \left[\left\{1 + \frac{N}{2[\{(K+L) - (4L - 1.9/K + L)\} + 2\{[(4L - 1.9/K) + L]0.5\}] - 0.55}\right\}^2 - 1.152\right]^4, \tag{2}$$

$$\begin{aligned}\text{taper} = {} & \left(\mathrm{V}\left(\mathrm{P} - \mathrm{N}/(\mathrm{N} - \mathrm{M} + \mathrm{L}/\mathrm{M}) + \mathrm{V}/(\mathrm{M} - \mathrm{N})^3 + (\mathrm{OV})/(\mathrm{M} - \mathrm{N})^3\right)\right) \\ & /(\mathrm{M} - \mathrm{N})^3 - \mathrm{V}(\mathrm{F} + \mathrm{G} + \left(\left(\mathrm{Q}\left(\mathrm{F} + \mathrm{H}^2\mathrm{Q}^2 - 1\right)^{0.25}\mathrm{Q}^2 + 2\mathrm{H}^2\mathrm{Q}^2 + 4\right)\right. \\ & /\left(3\mathrm{Q} - 3 - 2\mathrm{F} - 2\mathrm{G} - 2\left(\mathrm{F} + \mathrm{H}^2\mathrm{Q}^2 - 1\right)^{0.25}\mathrm{Q}^2 + 2\mathrm{H}^2\mathrm{Q}^2 + \mathrm{HQ} + 5\right) - 2v3 + 0.73\Big) \\ & /\left(\left(3\mathrm{Q} - 3 - 2\mathrm{F} - 2\mathrm{G} - 2\left(\mathrm{F} + \mathrm{H}^2\mathrm{Q}^2 - 1\right)^{0.25}\mathrm{Q}^2 + 2\mathrm{H}^2\mathrm{Q}^2 + \mathrm{HQ} + 5\right) - \mathrm{H}^2\mathrm{Q}^2 - 1\right) \\ & /\left((\mathrm{M} - \mathrm{N})^3\left(\mathrm{P} - \mathrm{N}/(\mathrm{N} - \mathrm{M} + \mathrm{L}/\mathrm{M}) + \mathrm{V}/(\mathrm{M} - \mathrm{N})^3 + (\mathrm{OV})/(\mathrm{M} - \mathrm{N})^3\right)\right) + 1.05,\end{aligned} \tag{3}$$

$$\text{heat affected zone} = \left[\frac{(1.22L/I) - 0.682}{v1v3}\right] - 0.079 - \left[\frac{1.22F}{G} - \frac{0.5356G}{v0}\right] + \frac{(1.22L/I) - 0.682}{v1}. \tag{4}$$

Appendixes A, B, C, and D show further details related to the derivation of the circularity, spatter, taper, and heat affected zone, respectively.

Comparison of the experimental and predicted outputs using the mathematical model obtained from GP is shown in Tables 2–5 for circularity, taper, spatter, and HAZ of pulsed

Table 2: Comparison between experimental and predicted values of circularity at R^2 = 99.68.

No.	PP (W) (v_0)	PF (Hz) (v_1)	AGP (kg/cm^2) (v_2)	PW (ms) (v_3)	Circularity (mm) Experimental	Circularity (mm) GP	Error %
1	250	210	12	0.4	0.908	0.908066	−6.6E − 05
2	210	210	8	0.2	0.9032	0.903074	0.000126
3	240	220	12	0.4	0.911	0.911254	−0.00025
4	210	210	8	0.6	0.953	0.953124	−0.00012
5	250	220	8	0.6	0.9425	0.941842	0.000658
6	210	250	12	0.6	0.978	0.978011	−1.1E − 05
7	210	230	10	0.4	0.948	0.945836	0.002164
8	230	210	10	0.6	0.957	0.958292	−0.00129
9	210	230	10	0.3	0.923	0.922506	0.000494
10	240	210	11	0.3	0.892	0.89308	−0.00108
11	220	210	9	0.3	0.926	0.926227	−0.00023
12	230	230	12	0.3	0.92	0.920843	−0.00084
13	240	220	12	0.3	0.9205	0.920919	−0.00042
14	220	250	8	0.3	0.896	0.895994	6.11E − 06
15	230	210	10	0.5	0.947	0.94698	1.96E − 05
16	240	230	8	0.4	0.899	0.898971	2.94E − 05
17	240	210	11	0.2	0.892	0.893078	−0.00108
18	220	240	12	0.6	0.974	0.973441	0.000559
19	240	250	10	0.6	0.954	0.955555	−0.00155
20	250	250	11	0.4	0.92	0.919789	0.000211
21	250	240	10	0.2	0.894	0.893536	0.000464
22	230	250	9	0.5	0.953	0.949875	0.003125
23	210	250	12	0.5	0.958	0.963079	−0.00508
24	250	240	10	0.3	0.892	0.893537	−0.00154
25	250	220	8	0.5	0.938	0.933247	0.004753
26	250	250	11	0.3	0.895	0.903726	−0.00873
27	230	230	12	0.2	0.893	0.892581	0.000419
28	230	220	11	0.2	0.89	0.892581	−0.00258
29	240	240	9	0.6	0.95	0.949358	0.000642
30	220	240	12	0.2	0.893	0.892039	0.000961
31	250	230	9	0.2	0.896	0.896958	−0.00096
32	220	220	10	0.5	0.951	0.950144	0.000856
33	240	240	9	0.5	0.95	0.943263	0.006737
34	210	220	9	0.2	0.9	0.896232	0.003768
35	220	250	8	0.2	0.902	0.896907	0.005093
36	250	210	12	0.5	0.948	0.94813	−0.00013
37	220	220	10	0.4	0.936	0.923214	0.012786
38	230	240	8	0.3	0.901	0.90405	−0.00305
39	250	230	9	0.6	0.9475	0.947726	−0.00023
40	230	250	9	0.4	0.911	0.928516	−0.01752
41	240	250	10	0.2	0.895	0.895507	−0.00051
42	220	210	9	0.4	0.91	0.90617	0.00383
43	240	230	8	0.5	0.94	0.936347	0.003653
44	210	240	11	0.5	0.951	0.959169	−0.00817
45	220	230	11	0.5	0.95	0.954643	−0.00464
46	220	230	11	0.6	0.97	0.967844	0.002156
47	230	240	8	0.4	0.901	0.906892	−0.00589
48	230	220	11	0.6	0.966	0.964493	0.001507
49	210	240	11	0.4	0.93	0.943397	−0.0134
50	210	220	9	0.3	0.922	0.918336	0.003664

PP: pulse power (W), PF: pulse frequency (Hz), PW: pulse width (ms), AGP: assist gas pressure (Kg/cm^3).

Nd:YAG laser microhole drilling of MMC components. Errors in determining predicted outputs are very few, and the percentage of error is less than ±1% which shows that results obtained from a GP mathematical model are highly acceptable.

Furthermore, Figure 2 shows the regression fit for the percentage of microdrilling process parameters of the MMCs. Figure 3 shows the experimental-predicted relationship of circularity, HAZ, taper, and spatter with the normal distribution behaviour. The models generated by the genetic programming perform better based on statistical terms and the historical dataset (training, validation, and applied data) to exhibit a better predictive capacity on the experimental dataset. The analysis of the mathematical expression of the GP

Table 3: Comparison between experimental and predicted values of HAZ at $R^2 = 99.88$.

No.	PP (W) (v_0)	PF (Hz) (v_1)	AGP (kg/cm^2) (v_2)	PW (ms) (v_3)	HAZ (mm)		Error %
					Experimental	GP	
1	240	230	8	0.4	0.04	$4.19E-02$	−0.00188
2	230	210	10	0.5	0.112	0.107232	0.004768
3	230	230	12	0.3	0.068	$7.13E-02$	−0.00328
4	210	230	10	0.3	0.068	$7.17E-02$	−0.00368
5	220	240	12	0.2	0.081	$8.02E-02$	0.000789
6	240	220	12	0.3	0.078	$7.82E-02$	−0.00023
7	220	210	9	0.4	0.088	$8.75E-02$	0.000453
8	250	220	8	0.6	0.104	0.103178	0.000822
9	210	210	8	0.2	0.065	$6.80E-02$	−0.00305
10	250	210	12	0.4	0.1	$9.97E-02$	0.000311
11	210	230	10	0.4	0.069	$7.04E-02$	−0.00139
12	240	220	12	0.4	0.073	$7.20E-02$	0.00103
13	230	220	11	0.6	0.085	$8.46E-02$	0.000417
14	220	250	8	0.3	0.102	0.101978	$2.21E-05$
15	220	230	11	0.6	0.089	$8.67E-02$	0.002272
16	220	220	10	0.5	0.094	$9.50E-02$	−0.00098
17	240	240	9	0.6	0.105	0.102995	0.002005
18	240	210	11	0.2	0.085	$8.12E-02$	0.003847
19	220	250	8	0.2	0.0747	$7.28E-02$	0.001893
20	230	250	9	0.5	0.1	0.103908	−0.00391
21	210	220	9	0.3	0.082	$8.05E-02$	0.001512
22	210	250	12	0.5	0.0909	$9.14E-02$	−0.00051
23	210	250	12	0.6	0.0921	$9.28E-02$	−0.00071
24	220	210	9	0.3	0.101	0.101721	−0.00072
25	240	240	9	0.5	0.1	0.10225	−0.00225
26	230	250	9	0.4	0.094	$9.11E-02$	0.002885
27	240	250	10	0.6	0.096	$9.56E-02$	0.000406
28	250	210	12	0.5	0.097	$9.83E-02$	−0.00131
29	230	230	12	0.2	0.076	$7.74E-02$	−0.0014
30	220	230	11	0.5	0.092	$9.06E-02$	0.001379
31	210	240	11	0.4	0.072	$7.25E-02$	−0.00049
32	230	210	10	0.6	0.095	$9.25E-02$	0.002548
33	250	250	11	0.3	0.078	$7.72E-02$	0.000826
34	250	220	8	0.5	0.105	0.104177	0.000823
35	210	220	9	0.2	0.084	$7.68E-02$	0.007168
36	220	240	12	0.6	0.095	$9.20E-02$	0.003025
37	230	240	8	0.4	0.055	$4.67E-02$	0.008281
38	210	210	8	0.6	0.1	$9.79E-02$	0.002054
39	250	230	9	0.2	0.07	$7.45E-02$	−0.00448
40	240	250	10	0.2	0.095	$8.29E-02$	0.012098
41	240	210	11	0.3	0.08	$7.90E-02$	0.001025
42	230	240	8	0.3	0.09	$8.87E-02$	0.001309
43	210	240	11	0.5	0.084	$9.04E-02$	−0.00638
44	250	240	10	0.3	0.065	$7.74E-02$	−0.01241
45	250	230	9	0.6	0.095	$9.90E-02$	−0.00402
46	250	250	11	0.4	0.08	0.081854	−0.00185
47	230	220	11	0.2	0.077	0.0783	−0.0013
48	220	220	10	0.4	0.075	0.07292	0.00208
49	250	240	10	0.2	0.091	$8.82E-02$	0.002776
50	240	230	8	0.5	0.09	0.090104	−0.0001

Model suggests specific laser output quality characteristics for the experimental system under various control factors that can be associated with the performance of a laser microdrilled hole in MMCs. The models generated by genetic programming allow representation of the experimental data without a detailed knowledge of the phenomenon. In addition, their study allows us to obtain a deeper insight into the relevant factors in describing the quality phenomenon; for instance, changes in any of the factors observed in quality of the microhole produced that might be associated with changes in the performance of hole production in MMC.

5. Conclusions

In this present work, new models of the circularity, spatter, heat affected zone, and taper of MMCs drilling properties at

Table 4: Comparison between experimental and predicted values of taper at R^2 = 99.43.

No.	PP (W) (v_0)	PF (Hz) (v_1)	AGP (kg/cm^2) (v_2)	PW (ms) (v_3)	Taper (deg)		Error %
					Experimental	GP	
1	230	250	9	0.4	3.5	3.48E + 00	0.020539
2	230	240	8	0.4	3.702	3.68349	0.01851
3	210	220	9	0.3	3.815	3.816499	−0.0015
4	230	210	10	0.5	3.75	3.72E + 00	0.034738
5	240	250	10	0.2	4.135	4.12E + 00	0.017045
6	210	240	11	0.4	3.45	3.43E + 00	0.023249
7	230	230	12	0.3	3.925	3.86E + 00	0.064339
8	220	240	12	0.6	3.5	3.487621	0.012379
9	220	240	12	0.2	4.12	4.13E + 00	−0.00979
10	240	220	12	0.3	3.8	3.81E + 00	−0.00709
11	230	240	8	0.3	3.8	3.79E + 00	0.010771
12	220	250	8	0.3	3.962	3.96E + 00	0.006659
13	230	220	11	0.2	4.16	4.16E + 00	−0.00037
14	240	220	12	0.4	3.775	3.757363	0.017637
15	250	230	9	0.6	3.8	3.770205	0.029795
16	210	210	8	0.6	4.2	4.200192	−0.00019
17	230	220	11	0.6	3.75	3.718309	0.031691
18	220	250	8	0.2	4.05	4.10E + 00	−0.04831
19	250	210	12	0.4	4.1	3.96E + 00	0.138649
20	250	220	8	0.5	3.5	3.522696	−0.0227
21	240	240	9	0.5	3.4	3.41E + 00	−0.01021
22	210	210	8	0.2	4.1	4.10E + 00	0.00162
23	240	230	8	0.5	3.505	3.523799	−0.0188
24	210	230	10	0.4	3.58	3.633331	−0.05333
25	220	210	9	0.3	3.6	3.774172	−0.17417
26	250	250	11	0.3	3.8	3.846722	−0.04672
27	210	240	11	0.5	3.307	3.441274	−0.13427
28	250	240	10	0.2	4.1	4.105488	−0.00549
29	220	230	11	0.5	3.3	3.441037	−0.14104
30	240	250	10	0.6	3.8	3.81E + 00	−0.00654
31	230	210	10	0.6	3.305	3.638603	−0.3336
32	230	250	9	0.5	3.38	3.41E + 00	−0.03093
33	230	230	12	0.2	4.05	4.110147	−0.06015
34	210	220	9	0.2	4	4.125376	−0.12538
35	250	230	9	0.2	4.15	4.123817	0.026183
36	240	240	9	0.6	3.75	3.748872	0.001128
37	240	210	11	0.3	3.9	3.86E + 00	0.043294
38	250	210	12	0.5	3.65	3.501807	0.148193
39	210	250	12	0.6	3.25	3.47E + 00	−0.21634
40	210	250	12	0.5	3.45	3.49592	−0.04592
41	220	220	10	0.5	3.6	3.572536	0.027464
42	240	210	11	0.2	3.95	4.11E + 00	−0.16276
43	250	220	8	0.6	3.6	4.114297	−0.5143
44	220	220	10	0.4	3.8	3.694675	0.105325
45	250	250	11	0.4	3.9	3.655343	0.244657
46	240	230	8	0.4	3.6	3.615975	−0.01597
47	220	230	11	0.6	3.4	3.677536	−0.27754
48	220	210	9	0.4	3.5	3.48E + 00	0.023193
49	250	240	10	0.3	3.8	3.80E + 00	0.004566
50	230	250	9	0.4	3.5	3.48E + 00	0.020539

different laser operating parameters are generated using Discipulus GP software and C programming. Using GP-based mathematical models, quality of laser drilled hole properties for MMCs involving various laser input parameters is determined quickly by substitution of laser input conditions, and without conducting any experiments, the actual results can be predicted. The comparison between the new GP-based model and the experimental results indicated that the new model is more accurately close to ± 0.006 to 0.009. Therefore, the new model can be considered an alternative method to estimate the mechanical properties when the experimental measurements or correlations are not available. The correctness of solutions achieved by GP depends on correlated evolutionary parameters, the number of experimental results, and their level of accuracy. To improve the structure of the model during evolution,

Table 5: Comparison between experimental and predicted values of spatter at R^2 = 99.3.

No.	PP (W) (v_0)	PF (Hz) (v_1)	AGP (kg/cm^2) (v_2)	PW (ms) (v_3)	Spatter (mm) Experimental	Spatter (mm) GP	Error %
1	220	220	10	0.4	0.055	5.49E − 02	0.00013
2	230	220	11	0.6	0.044	4.42E − 02	−0.00018
3	210	250	12	0.6	0.044	4.34E − 02	0.000648
4	240	220	12	0.3	0.043	4.32E − 02	−0.00022
5	230	240	8	0.3	0.04	4.36E − 02	−0.00365
6	210	230	10	0.3	0.042	4.21E − 02	−7.3E − 05
7	250	240	10	0.2	0.065	6.50E − 02	3.18E − 05
8	230	230	12	0.2	0.043	4.31E − 02	−7.8E − 05
9	240	240	9	0.6	0.072	7.16E − 02	0.000406
10	230	220	11	0.2	0.045	4.50E − 02	−1.6E − 05
11	250	230	9	0.2	0.068	6.82E − 02	−0.00024
12	220	240	12	0.6	0.052	5.23E − 02	−0.00028
13	210	250	12	0.5	0.043	4.29E − 02	6.36E − 05
14	220	210	9	0.4	0.059	5.94E − 02	−0.00045
15	210	220	9	0.2	0.0445	0.044101	0.000399
16	220	240	12	0.2	0.05	5.02E − 02	−0.00019
17	230	210	10	0.5	0.072	7.03E − 02	0.001661
18	230	240	8	0.4	0.071	6.97E − 02	0.001265
19	240	210	11	0.2	0.056	5.54E − 02	0.000566
20	230	250	9	0.5	0.074	7.25E − 02	0.001524
21	240	230	8	0.4	0.075	0.064522	0.010478
22	220	250	8	0.3	0.074	0.071546	0.002454
23	250	210	12	0.5	0.046	5.18E − 02	−0.00581
24	210	240	11	0.4	0.043	4.20E − 02	0.000993
25	230	210	10	0.6	0.049	5.21E − 02	−0.00307
26	250	250	11	0.3	0.065	5.50E − 02	0.010003
27	210	230	10	0.4	0.04	4.28E − 02	−0.00277
28	210	210	8	0.6	0.043	0.042277	0.000723
29	210	240	11	0.5	0.045	0.044648	0.000352
30	220	230	11	0.6	0.057	5.40E − 02	0.003045
31	240	220	12	0.4	0.042	4.29E − 02	−0.00093
32	240	250	10	0.2	0.066	6.64E − 02	−0.00042
33	230	230	12	0.3	0.041	4.27E − 02	−0.00171
34	230	250	9	0.4	0.069	6.84E − 02	0.000556

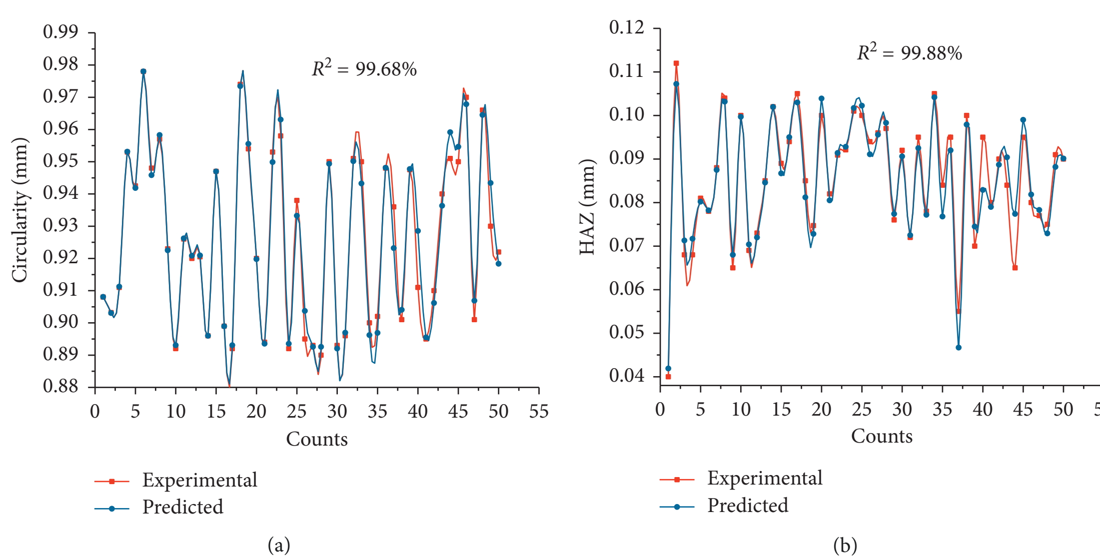

Figure 2: Continued.

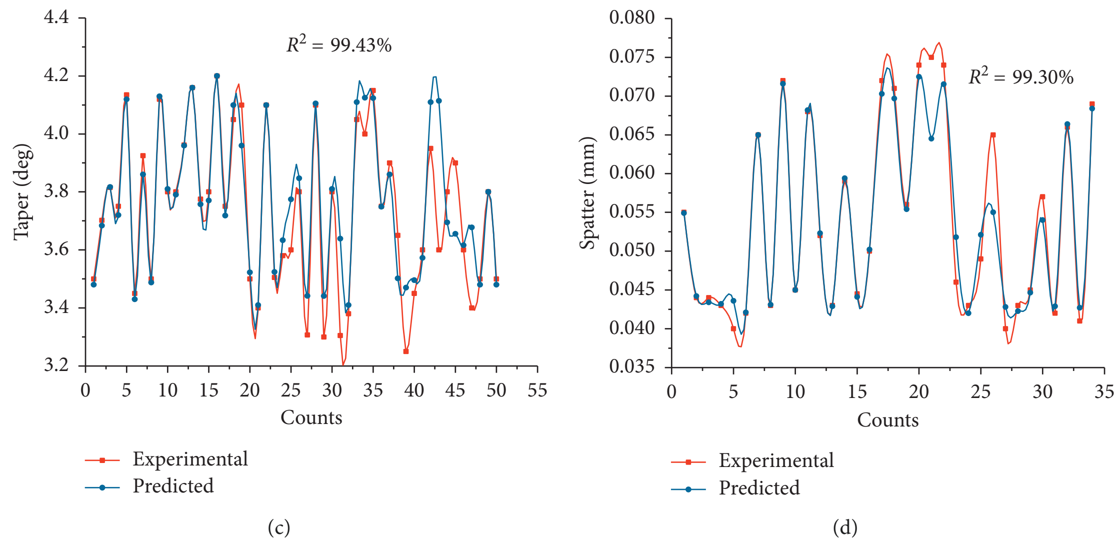

FIGURE 2: Regression fit for the percentage of microdrilling process parameters of the MMCs. (a) Experimental-predicted value of circularity. (b) Experimental-predicted value of HAZ. (c) Experimental-predicted value of taper. (d) Experimental-predicted value of spatter.

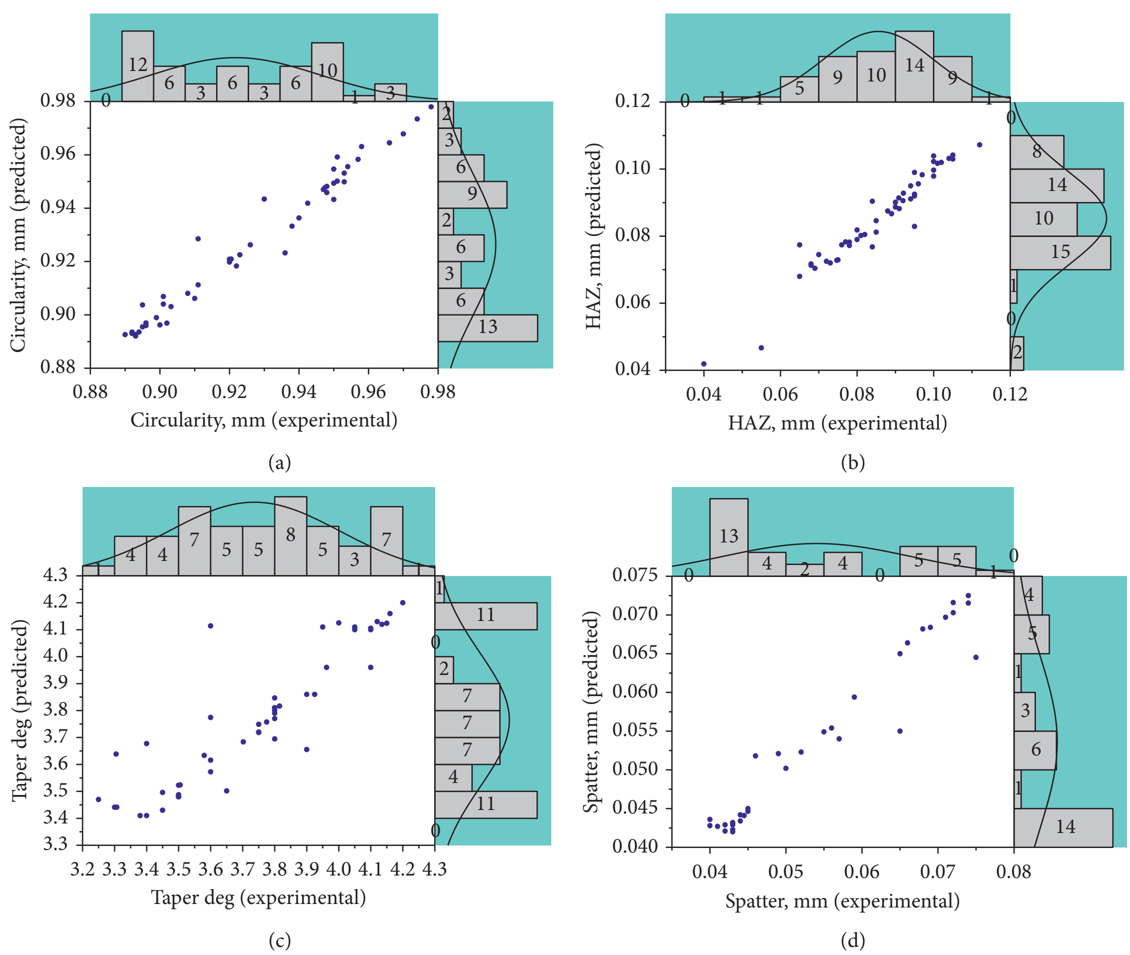

FIGURE 3: Experimental-predicted relationship of (a) circularity, (b) HAZ, (c) taper, and (d) spatter.

more information was supplied through experimental measurements. Therefore, the proposed mathematical model has verified its results are adaptable up to reliability of 99.3 to 99.8% to forecast experimental results. In the testing stage, the GP model gives the same result as was found out during the experiment with the reliability of cent percent. The GP approach has thus proved to be a highly skilled and advantageous tool for recognizing correlations in data when no proper theoretical or other methods are possible or available.

Appendix

A. Circularity

$$\begin{aligned} A = {} & ((0.954v0 + (2v2 + 0.1644)^2 (v2 + 0.1644)^2 - (4503599627370496 (2v3 - v0 + (4v2 + 0.6576) (v2 + 0.1644) \\ & + (2v2 + 0.1644) (v2 + 0.1644))^2)/4720808237398575 - (2v2 + 0.1644) (v2 + 0.1644))) \\ & \cdot (2 (2v2 + 0.1644)^2 (v2 + 0.1644)^2 - (9007199254740992 (2v3 - v0 + (4v2 + 0.6576) (v2 + 0.1644) \\ & + (2v2 + 0.1644) (v2 + 0.1644))^2)/4720808237398575 + 2v0v3)^{-1}, \end{aligned} \quad (A.1)$$

$$B = \frac{A}{\left(\left(\left\{\left(\left(\left(\left[A3\left(\left((v0/v1v3)^2 - (71143/40000)\right)2A^2 - 2\right)\right)0.74\right]/v2\right)\right] + 1.92\right)^2 + 2A\right\} + v1\right]v3/v1\right)} + 0.9045, \quad (A.2)$$

$$C = \left[\frac{1}{(B - 2B^7)}\right] * \left[\left[\left\{2B^7\right\} - 1.35\right]2v3\right], \quad (A.3)$$

$$D = \left\{\left[-\left(\left\{\left(\left[(4B)^3 - 1.35\right]4v3^2\right) - \left(\frac{2}{B} - 4B^6\right) + 2C\right\} - 1.1\right)0.24\right] + 1.08\right\}v3, \quad (A.4)$$

$$E = 382Dv3v2C^2 - (2v1 + v0 + 2v2)^2 DC + \frac{(382Dv3v2C^2 - 2v1 + v0)}{E^2} + v2, \quad (A.5)$$

$$F = \frac{C}{DC^2} + \frac{(382Dv3v2C^2 - 2 * v1 + v0)DC}{E2} + 382Dv3v2C^2 - 2v1 + v0, \quad (A.6)$$

$$G = \left(\frac{E^2}{(1/C) + 382Dv3v2C^2 - 2v1 + v0} + 2v0 - 15F + 11v2\right)1.08 - \mathrm{v}1. \quad (A.7)$$

B. Spatter

$$A = \frac{\left[0.2454 (8.272\{0.2454 + v2\} - 0.7335 + v3)^8 - 0.18\right]}{\left[0.2454 (8.272\{0.2454 + v2\} - 0.7335 + v3)^8 - 0.1732\right]}, \quad (B.1)$$

$$\begin{aligned} B = {} & \left[0.2454(8.272\{0.2454 + v2\} - 0.7335 + v3)^8 - 0.1732\right] \\ & + \left\{\frac{1}{\left\{\left[0.2454 (8.272\{0.2454 + v2\} - 0.7335 + v3)^8 - 0.1732\right] - (A^2 - 0.56)\right\}^4} - 0.442\right\}^2, \end{aligned} \quad (B.2)$$

$$C = \left\{\frac{1 + v0}{B}\right\}^2 \left\{0.2454 \frac{1}{\left\{\left(B/\left\{\left[0.2454 (8.272\{0.2454 + v2\} - 0.7335 + v3)^8 - 0.1732\right] - (A^2 - 0.56)\right\}^4\right) - 0.442\right\}^2}\right\}, \quad (B.3)$$

$$D = \frac{0.2454}{\left\{\left(B/\left\{\left[0.2454\left(8.272\{0.2454 + v2\} - 0.7335 + v3\right)^8 - 0.1732\right] - \left(A^2 - 0.56\right)\right\}^4\right) - 0.442\right\}^2} - C + 0.96, \tag{B.4}$$

$$E = \frac{\left[\left(D/\left\{4\left[\left(\{B - (1 + v0/B)\}/D\right)\right]^2 - 0.256 - D\right\}\right)\right]}{\left[\left\{4\left[\left(\{B - (1 + v0/B)\}/D\right)\right]^2 - 0.256 - D\right\}^2 - 1\right]}, \tag{B.5}$$

$$F = \left\{B - \frac{(1 + v0)}{B}\right\} + D\left[C - \frac{0.96}{\{B - ((1 + v0)/B)\}}\right] + \frac{\left[(2.8 - v2)^2/E\right]}{\left\{\left[\{B - (1 + v0/B)\} + D\left[C - (0.96/\{B - (1 + v0/B)\})\right]\right]^2 + v3\right\}}, \tag{B.6}$$

$$G = 2\frac{\left[(2.8 - v2)^2/E\right]}{\left[\{B - (1 + v0/B)\} + D\left[C - (0.96/\{B - (1 + v0/B)\})\right]\right]^2} + 2v3 + 2E + 2, \tag{B.7}$$

$$H = 2\frac{(2.8 - v2)^2/E}{\left[\{B - (1 + v0/B)\} + D\left[C - (0.96/\{B - (1 + v0/B)\})\right]\right]^2 + 2v3 + 3E + 3} \tag{B.8}$$

$$x = H\frac{\{2G\}^{0.5}}{F + G}, \tag{B.9}$$

$$I = H + \left(H\frac{\left(\{v2\left[(F + G) + x\right] + 2\left[2x\right]\}/\{2\left[2x\right] - \left[(F + G) + x\right]\}\right)}{\left[(F + G) + x\right]} - [x]\right), \tag{B.10}$$

$$J = \frac{\left(\left\{\left[(F + G) + x\right] - [2x] + 2\left\{(H/IH) + \left(\{IH/H\}/\left[\left[(F + G) + x\right] - [2x]\right]\right)\right\} - 0.446\right)\right\} - 0.316\right)^2}{\left[(F + G) + x\right] - [2x] + 2\left\{\dfrac{H}{IH} + \left(\{IH/H\}/\left[\left[(F + G + x)\right] - [2x]\right]\right)\right\} - 0.446}, \tag{B.11}$$

$$K = \left[(F + G) + x\right] - [2x] + 2\left\{\frac{H}{IH} + \frac{\{IH/H\}}{\left[\left[(F + G) + x\right] - [2x]\right]}\right\} - 0.446 + J, \tag{B.12}$$

$$L = 1.2698 - \frac{K}{K} - \frac{H}{IH} + \frac{\left(\left\{\left(IH/H/\left[\left[(F + G) + x\right] - [2x]\right]\right)\right\} - 0.446\right)}{\left[\left[(F + G) + x\right] - [2x]\right]}, \tag{B.13}$$

$$M = \left\{2\left[\frac{4L - 1.9}{K + L}\right]^{0.5}\right\} + v0 - 2\left[\left\{(K + L) - \frac{4 * L - 1.9}{K + L}\right\} + 2 * \left\{\left[\frac{4 * L - 1.9}{K + L}\right]^{0.5}\right\}\right], \tag{B.14}$$

$$\begin{aligned} N = {} & \frac{H}{IH} + \frac{\left(\left\{(IH/H)/\left[\left[(F + G) + x\right] - [2x]\right]\right\} - 0.446\right)\right)}{\left[\left[(F + G) + x\right] - [2x]\right]} \\ & + \frac{\left(M/\left(M + 2v2 - 0.153\right)^2\right)}{\left\{2V2\left[\{(K + L) - (4L - 1.9/K + L)\} + 2\left[\left[(4L - 1.9)/(K + L)\right]^{0.5}\right]\right]\right\}}. \end{aligned} \tag{B.15}$$

C. Taper

$$\left(M - N - \frac{L}{M} + \frac{N}{N - M + (L/M)}\right)^4 = V, \tag{C.1}$$

$$\begin{aligned}Q &= (A - 6C + 0.002v3 + 1)A \\ &= ((4508098723398239)/(4503599627370496v2 - 9007199254740.992v3 + 4512597819425982)) - 0.001v3 + (2263) \\ &\quad /((10000 * v0 + 54.2v3 - 4607074332408960516096 00)/(9007199254740.992v3 - 9382184668271360000)) \\ &\quad +\Big((0.001v3 - 0.001)(1.001v3 - 0.001)^{0.5}(195.28v3 - 175.55 + 9989) - 0.091\Big)/(4508098723398239) \\ &\quad /(4503599627370496v2 - 9007199254740.992v3 + 4512597819425982) - 0.001v3 \\ &\quad + ((2263)/(10000v0 + 54.2v3 - 460707433240896051609600/(9007199254740.992v3 - 9382184668271360000)) \\ &\quad +\Big((0.001v3 - 0.001)(1.001v3 - 0.001)^{0.5}195.28v3 - 175.55 + 9989\Big) - 0.091),\end{aligned} \tag{C.2}$$

$$\begin{aligned}B &= 0.001v3 - A + \frac{9016197446796478}{(4503599627370496v2 - 9007199254740.992v3 + 4512597819425982)} \\ &\quad + \frac{4526}{(10000v0 + 54.2v3 - (460707433240896051609600/(9007199254740.992v3 - 938)))},\end{aligned} \tag{C.3}$$

$$\begin{aligned}C &= \frac{B^2 9.01 * 10^{15}}{4.51 * 10^{15}v2 - 9 * 10^{12}v3 + 4.51 * 10^{15}} - A \\ &\quad + \frac{4526}{10000v0 + 54.2v3 - 4.61 * 10^{23} + (0.001v3 – 1000)(1.001\text{v}3 – 1000)^{0.5}(195.26\text{v}3 - 175.5) + 1000} - 0.001,\end{aligned} \tag{C.4}$$

$$\begin{aligned}D &= \bigg((4526)/\bigg(10000v0 + \Big(54.2v3 - 46.07 * 10^{22}\Big)/\Big\{\Big(9 * 10^{12}v3 - 9.4 * 10^{18}\Big) + (0.001v3 - 1000)(1.001v3 - 1000)^{0.5} \\ &\quad \cdot (195.26v3 - 175.5) + 10000 - \Big(9.01 * 10^{15}/\Big(4.5 * 10^{15}v2 - 9 * 10^{12}v3 + 4.5 * 10^{15}\Big)\Big) \\ &\quad - A + (Q + 1)^{0.5}(Q + 4C) - 0.001\Big\}\bigg)\bigg)^{-1},\end{aligned} \tag{C.5}$$

$$\begin{aligned}E &= 6C - \Big(A - 0.001v3 - 10.18 * 10^{15}\Big)\Big(22.52 * 10^{16}v0 + 12.2 * 10^{16}v3 - 1038 * 10^{36}/\Big(10.43 * 10^{18}v3 - 9.4 * 10^{18}\Big) \\ &\quad + \Big(2.252v3 - 2.25 * 10^{18}\Big)(1.001v3 - 1000)^{0.5}(195.26v3 - 175.5) + 2.252 * 10^{19} - 40.62 * 10^{31} \\ &\quad /\Big(10.41v2 - 20.3 * 10^{27}v3 + 10.2 * 10^{30}\Big) - 4.5 * 10^{15}/\Big(4.5 * 10^{14}v2 - 9 * 10^{12}v3 + 4.5 * 10^{15}\Big) - 2263/10000v0 \\ &\quad + 195.26v3 - 4.61 * 10^{21}/\Big(9 * 10^{12}v3 - 9.4 * 10^{18}\Big) + (0.001v3 - 0.001)(1.001v3 - 0.001)^{0.5} \\ &\quad \cdot (195.26v3 - 175.55 + 9989) + \Big(D^{0.5}Q\Big)\Big)^{-1},\end{aligned} \tag{C.6}$$

$$\begin{aligned}F &= \Big(\Big(4.51 * 10^{15}\Big)/\Big(4.5 * 10^{14}v2 - 10.43 * 10^{18}v3 + 4.51 * 10^{15}\Big) - 0.001v3\Big) + (2263)/\Big(10000v0 + 54.2v3 - 4.6 * 10^{23}\Big) \\ &\quad /\Big(10.43 * 10^{18}v3 – 9.4 * 10^{18}\Big) + (0.001v3 - 0.001)(1.001v3 - 0.001)^{0.5}(195.27v3 - 175.55 + 9989) \\ &\quad - \Big(v3 + E^2\Big(4.51 * 10^{15}\Big)/\Big(4.5 * 10^{15}v2 – 10.43 * 10^{18}\text{v}3 + 4.51 * 10^{15}\Big) - 0.001v3\Big) + (2263) \\ &\quad /\bigg(10000v0 + 54.2v3 - 4.61 * 10^{27}/\Big(10.43 * 10^{18}v3 - 9.4 * 10^{18}\Big) + \bigg((0.001v3 - 0.001)(1.001v3 - 0.001)^{0.5} \\ &\quad \cdot (195.27v3 - 175.55 + 9989)\bigg)^2\bigg)/\Big(Q^8 - 0.73\Big)\text{Q},\end{aligned} \tag{C.7}$$

$$\begin{aligned}G &= -\Big(v3 + E^2\Big(\Big(4.51 * 10^{15}\Big)/\Big(4.5 * 10^{15}v2 – 9.01 * 10^{12}v3 + 4.51 * 10^{14}\Big)\Big) - 0.001v3 + (2263)/10000v0 + 54.2v3 \\ &\quad - \Big(\Big(4.61 * 10^{27}\Big)/\Big(9.01 * 10^{12}v3 - 9.4 * 10^{18}\Big)\Big) + (0.001v3 - 0.001)(1.001v3 - 0.001)^{0.5} \\ &\quad \cdot (1000000000v3 - 899000000)/(5121169) + 9989\Big)^2/\Big(Q^8 - 0.73\Big)Q - Q^2A - 9.02 * 10^{15} \\ &\quad /\Big(4.5 * 10^{15}v2 - 9.01 * 10^{12}\text{v}3 + 4.51 * 10^{15}\Big) - \Big((4526)/\Big(10000v0 + 54.2v3 - 4.61 * 10^{27}/10^{18} * (10.5v3 - 9.4)\Big)\Big) \\ &\quad + \Big((0.001v3 - 1000)(1.001 * v3 - 1000)^{0.5}(195.26v3 - 175.55) + 9989 + 0.001\Big)/E^2,\end{aligned} \tag{C.8}$$

$$H = v3 + \Big(\Big(\Big(E^2\big(4.51 * 10^{15}\big)/\Big(\big(4.5 * 10^{15} v2 - 11.26 * 10^{14} v3\big)/125 + 4.51 * 10^{15}\Big)\Big)\Big) - (v3/1000)\Big) + (2263)$$
$$/\Big(\big(10000 * v0 + 54.2v3 - 46.1 * 10^{22}/10^{18} * ((10.5v3 - 9.4))\big)\Big) + \big((0.001v3 - 0.001)(1.001v3 - 0.001)^{0.5}$$
$$\cdot \big(10^9 v3 - 8.99 * 10^8\big)\big)\Big(\big((5121169 + 10000)2/\big(Q^8 - 0.73\big)Q + F\big)\Big)^{-1}, \quad \text{(C.9)}$$

$$I = \Big(6A - 36C - 8F - 8G + \Big(\Big(8v3 - \Big(\Big(8Q - 16F - 8G + 8 - 8\big((HQ)^2 - 2\big)^{0.25} Q^2 + 4H^2Q^2 + 8\Big)/3Q + 3 - 2F - 2G$$
$$- 2\big(F + (HQ)^2 - 1\big)^{0.25} Q^2 + 2H^2Q^2 + HQ + 5\Big) - 8v3 + 2.92\Big)/\Big(3Q - 2F - 2G + 3 - 2\big((HQ)^2 - 1\big)^{0.25}$$
$$\cdot Q^2 + 2(HQ)^2 + HQ + 5\Big)^{-1}\Big) - 4\big(F + (HQ)^2 - 1\big)^{0.25} Q^2 + 8(HQ)^2 - \Big(\Big(4Q + 4 - 4F - 4G\big(F + (HQ)^2 - 1\big)^{0.5}$$
$$\cdot Q^2 + 4(HQ)^2 + 8\Big)/\Big(3Q + 3 - 2F - 2G - 2\big(F + (HQ)^2 - 1\big)^{0.25} Q^2 + 2(HQ)^2 + HQ + 5\Big)\Big)^{-1} + 2Q + 12.54\Big)^{0.5}, \quad \text{(C.10)}$$

$$J = \Big(2A - 12C - 2F - 2G + 2I + 0.004v3 - 2\big(F + H^2Q^2 - 1\big)^{1/4} Q^2 + 2H^2Q^2 + 4\Big)^{1/2}$$
$$- \frac{J}{\big(2A - 12C - 2F - 2G + 2I + (v3/250) - 2(F + H^2Q^2 - 1)^{0.25} Q^2 + 2H^2Q^2 + 4\big)}, \quad \text{(C.11)}$$

$$K = (2Q - 2F - 2G + 2I - 4)\big(F + H^2Q^2 - 1\big)^{0.25} Q^2 + 2H^2Q^2 + 4^{0.5}$$
$$- \frac{(2J)}{\big((2Q - 2F - 2G + 2I - 4)(F + H^2Q^2 - 1)^{0.25} Q^2 + 2H^2Q^2 + 4\big)}, \quad \text{(C.12)}$$

$$L = \frac{J}{\big((2Q - 2F - 2G + 2I - 4)(F + H^2Q^2 - 1)^{0.25} Q^2 + 2H^2Q^2 + 4\big)1.5} - \frac{J}{(Q - F - G + I)(F + H^2Q^2 - 1)^{0.25} Q^2 + 2H^2(Q^2 + 4)}, \quad \text{(C.13)}$$

$$M = \frac{K - L + (2Q - 2F - 2G - 4)(F + H^2Q^{0.25}Q^2 + 2H^2Q^2 + 4)}{K}$$
$$- \frac{(2Q - 2F - 2G - 4)(F + H^2Q^2 - 1)^{0.25} Q^2 + 2H^2Q^2 + 4\big)}{K\big(K - L + (2Q - 2F - 2G - 4)(F + H^2Q^2 - 1)^{0.25}(Q^2 + 2H^2Q^2 + 4/K)\big)}, \quad \text{(C.14)}$$

$$N = \frac{\big((2Q - 2F - 2G - 4)(F + H^2Q^2 - 1)^{0.25} Q^2 + 2H^2Q^2 + 4\big)}{\big(KK - L + (2Q - 2F - 2G - Q^2 - 4)^{0.25}((Q^2 + 2H^2Q^2 + 4)/K)\big)} + \frac{(2L/M)}{M - (L/M)}, \quad \text{(C.15)}$$

$$O = \Big((-N/(N - M + (L/M)))/\Big(F + G + (2Q - 2F - 2G - 4)\big(F + H^2Q^2 - 1\big)^{0.25} Q^2 + 2H^2Q^2 + 4\Big)\Big)$$
$$\cdot \Big(\Big((3Q - 2F - 2G - 5)\big(F + H^2Q^2 - 1\big)^{0.25}\big(Q^2 + 2H^2Q^2 + HQ + 5\big) - (2v3 + 0.73)\Big)$$
$$/\Big((3Q - 2F - 2G - 5)\big(F + H^2Q^2 - 1\big)^{0.25}\big(Q^2 + 2H^2Q^2 + HQ - H^2Q^2 - 1\big)^3\Big)\Big)^{-1}, \quad \text{(C.16)}$$

$$P = \big(O/\big((M - N)^3/V\big)\big) \cdot \Big(\Big(\Big(F + G + \Big(\Big((2Q - 2F - 2G - 4)\big(F + H^2Q^{2.25} + 0.004H^2Qv3 + 1\big)^2 + 4\Big)$$
$$/\Big((3Q - 2F - 2G - 5)\big(F + (HQ)^2 - 1\big)^{0.25} Q^2\Big)\Big) + 2(HQ)^2 - 1\Big)^{0.25} Q^2 + 2(HQ)^2 + HQ + 5\Big) - (HQ)^2 - 1\Big)^{-1}. \quad \text{(C.17)}$$

D. Heat Affected Zone (HAZ)

$$A = 1.38v3\frac{(16306.51v2v3 + 14782.8v1v2)}{(v0v1)^2} - \frac{13.94v3}{v0v1^2} - \frac{4.14v3^2}{v1v0} - 1.38v3v2 + 0.4v3 + 1.725, \tag{D.1}$$

$$B = \frac{(2326.4v2v3 + 2109v1v2)}{v0v1} - \frac{3.366}{v1} + \frac{(16306.51v2v3 + 14782.8v1v2)}{(v0v1)^2} - \frac{10.1}{v0v1^2} - \frac{3v3}{v1v0} - v2 + 0.29, \tag{D.2}$$

$$\begin{aligned} C = {} & 2.73\left\{\left[\frac{18.44A}{v3^2} - 2v0\right]\left[\frac{5435.5v2v3 + 4927.6v1v2}{(v0v1)^2} - \frac{3.366}{v0v1^2} - \frac{0.92v3}{v1v0} + 1.09\right]\right\}^2 \\ & \cdot 0.92\left[-\frac{5435.5v2v3 + 4927.6v1v2}{(v0v1)^2} + \frac{3.1}{v0v1^2} + \frac{0.92v3}{v1v0} + 0.92A\right] - 0.121, \end{aligned} \tag{D.3}$$

$$D = \left(B + 2C\left\{\frac{-(5435.5v2v3 + 4927.6v1v2)}{(v0v1)^2} + \frac{3.366}{v0v1^2} + \frac{v3}{v1v0} + A\right\}\right) - 1, \tag{D.4}$$

$$E = \frac{\left(\left\{[0.741D + v3]^2 - 1\right\}^2 - 3.2\right)}{\left[\left(5435.5v2v3 + 4927.6v1v2/(v0v1)^2\right) - (3.366/v0v1^2) - (v3/v1v0) + 1.09\right]}, \tag{D.5}$$

$$\begin{aligned} F = {} & \left\{-\frac{5435.5v2v3 + 4927.6v1v2}{(v0v1)^2} + \frac{3.366}{v0v1^2} + \frac{v3}{v1v0} + A\right\}8C(E - v3) \\ & \cdot \left\{\frac{\left[\left(5435.5v2v3 + 4927.6v1v2/(v0v1)^2\right) - (3.366/v0v1^2) - (v3/v1v0) + 1.09\right]}{v0}\right\}^2, \end{aligned} \tag{D.6}$$

$$G = \left\{1.1\left(\left[\left(\left\{\left[\left\{(1-F)^4 - 1\right\}^2 - 1\right] + F\right\}^2 - 1 + F\right)^2 - 1\right]^4 - 1\right)^4 - 1.1\right\}^2, \tag{D.7}$$

$$\begin{aligned} H = {} & \left[\left\{D + 0.741D + v3 - \left\{[0.741D + v3]^2 - 1\right\}^2 + 1\right\} + E - 16.92(G/v0)\right] \\ & + \frac{(33.84(G/v0) - (6F/G) - 0.066)}{\left[\left\{D + 0.741D + v3 - \left\{[0.741D + v3]^2 - 1\right\}^2 + 1\right\} + E - 16.92(G/v0)\right](F/G)}, \end{aligned} \tag{D.8}$$

$$\begin{aligned} I = {} & \left[\frac{5435.5v2v3 + 4927.6v1v2}{(v0v1)^2} - \frac{3.366}{v0v1^2} - \frac{v3}{v1v0} + 1.09\right] \\ & - \frac{F(33.84(G/v0) - (6F/G) - 0.066)}{\left[\left\{D + 0.741D + v3 - \left\{[0.741D + v3]^2 - 1\right\}^2 + 1\right\} + E - 16.92(G/v0)\right]G}, \end{aligned} \tag{D.9}$$

$$J = \frac{(85.14G/v0 - 15.1F/G - 0.1662)}{\left[\left\{D + 0.741D + v3 - \left\{[0.741D + v3]^2 - 1\right\}^2 + 1\right\} + E - 16.92 * (G/v0)\right] * (F/G)}, \tag{D.10}$$

$$K = 2.5\frac{\{1 - [2JIH^3 + 2I/(Hv2)]\}}{\{[(F/G) - 0.44(G/v0)]I^2\}} + \frac{v2}{v0} + \left\{2JIH^3 + \frac{2I}{(Hv2)}\right\}, \tag{D.11}$$

$$L = \left[\left(\frac{v2\left\{\left[2v1\frac{K}{Iv0}\right]^2 - 1\right\}^2}{v0 - ([\{(2JIH^3 + 2I/Hv2)\}]/I)}\right) - v0 - 1.26\right]\left\{2JIH^3 + \frac{2I}{(Hv2)}\right\}. \tag{D.12}$$

Data Availability

The data used to support the findings of this study are available from the corresponding author upon request.

Conflicts of Interest

The authors have no conflicts of interest.

Authors' Contributions

MY and MSA participated in the conceptualization of the research, prepared the data for experimentation and the analysis and interpretation of the data. MY used Genetic program Discipulus software for the analysis, including writing equations. MY drafted the manuscript, and figures were sketched by MSA. MY and MSA revised the manuscript for intellectual content and approved the final manuscript.

References

[1] L. H. Manjunatha et al., "Development and comparative studies of aluminum-based carbon nano tube metal matrix composites using powder metallurgy and stir casting technology," *International Journal of Scientific and Engineering Research*, vol. 8, no. 2, pp. 521–526, 2017.

[2] M. Yunus, J. F. Rahman, and S. Ferozkhan, "Genetic programming approach for the prediction of thermal characteristics of ceramic coatings," *International Journal of Industrial Engineering Research and Development*, vol. 2, no. 1, pp. 69–79, 2011.

[3] A. S. Kuar, B. Doloi, and B. Bhattacharyya, "Modelling and analysis of pulsed Nd:YAG laser machining characteristics during micro-drilling of zirconia (ZrO_2)," *International Journal of Machine Tools and Manufacture*, vol. 46, no. 12, pp. 1301–1310, 2006.

[4] A. Manna and B. Bhattacharayya, "A study on machinability of Al/SiC-MMC," *Journal of Materials Processing Technology*, vol. 140, no. 1–3, pp. 711–716, 2003.

[5] K. H. Leong, "Drilling with lasers," in *Industrial Laser Solutions for Manufacturing*, pp. 36–42, Pennwell, Tulsa, OK, USA, 2000.

[6] J. Meijer, "Laser beam machining (LBM), state of the art and new opportunities," *Journal of Materials Processing Technology*, vol. 149, no. 1–3, pp. 2–17, 2004.

[7] M. Yunus, J. F. Rahman, and S. Ferozkhan, "Evaluation of machinability characteristics of industrial ceramic coatings using genetic programming based approach," *International Journal of Mechanical Engineering and Technology*, vol. 2, no. 2, pp. 126–137, 2011.

[8] J. R. Koza, *Genetic Programming: On the Programming of Computers by Natural Selection*, MIT Press, Cambridge, MA, USA, 1992.

[9] M. Yunus and M. S. Alsoufi, "Prediction of mechanical properties of plasma sprayed thermal barrier coatings (TBCs) with genetic programming (GP)," *International Journal of Engineering Trends and Technology*, vol. 47, no. 3, pp. 139–145, 2017.

[10] M. Ghoreishi, D. K. Y. Low, and L. Li, "Comparative statistical analysis of hole taper and circularity in laser percussion drilling," *International Journal of Machine Tools and Manufacture*, vol. 42, no. 9, pp. 985–995, 2002.

[11] M. V. Lakshmi and M. L. Chaitanya, "Application of taguchi based grey relational analysis for evaluating optimal parameters of laser micro-drilling Al7075/SiCp metal matrix composite," *International Journal of Mechanical Engineering and Technology*, vol. 5, no. 1, pp. 16–22, 2015.

[12] C. Bagger and F. O. Olsen, "Pulsed mode laser cutting of sheets for tailored blanks," *Journal of Materials Processing Technology*, vol. 115, no. 1, pp. 131–135, 2001.

[13] S. Bandyopadhyay, J. K. Sarin Sundar, G. Sundararajan, and S. V. Joshi, "Geometrical features and metallurgical characteristics of Nd:YAG laser drilled holes in thick IN718 and Ti–6Al–4V sheets," *Journal of Materials Processing Technology*, vol. 127, no. 1, pp. 83–95, 2002.

[14] B. S. Yilbas and Z. Yilbas, *Parameters Affecting Hole Geometry in Laser Drilling of Nimonic 75*, SPIE, Los Angeles, CA, USA, 1987.

[15] D. K. Y. Low, L. Li, A. G. Corfe, and P. J. Byrd, "Spatter-free laser percussion drilling of closely spaced array holes," *International Journal of Machine Tools and Manufacture*, vol. 41, no. 3, pp. 361–377, 2001.

[16] C. M. Sharp, R. E. Mueller, J. Murthy, M. H. McCay, and J. Cutcher, "A novel anti-spatter technique for laser drilling: applications to surface texturing," in *Laser Materials Processing*, pp. 41–50, Laser Institute of America, San Diego, CA, USA, 1997.

[17] M. Brezocnik, M. Kovacic, and M. Ficko, "Prediction of surface roughness with genetic programming," *Journal of Materials Processing Technology*, vol. 157-158, pp. 28–36, 2004.

[18] J. R. Koza, *Genetic Programming II (Automatic Discovery of Reusable Programs)*, The MIT Press, Cambridge, MA, USA, 1994.

[19] M. Brezocnik and M. Kovacic, "Integrated genetic programming and genetic algorithm approach to predict surface roughness," *Materials and Manufacturing Processes*, vol. 18, no. 3, pp. 475–491, 2003.

[20] L. Gusel and M. Brezocnik, "Modeling of impact toughness of cold formed material by genetic programming," *Computational Materials Science*, vol. 37, no. 4, pp. 476–482, 2006.

[21] S. R. Choi, D.-M. Zhu, and R. A. Miller, "Effect of sintering on mechanical and physical properties of plasma-sprayed thermal barrier coatings," NASA/TM-2004-212625, NASA, Washington, DC, USA, 2004.

[22] Y. S. Chang, K. S. Park, and B. Y. Kim, "Nonlinear model for ECG R-R interval variation using genetic programming approach," *Future Generation Computer Systems*, vol. 21, no. 7, pp. 1117–1123, 2005.

[23] M. Brezocnik and L. Gusel, "Predicting stress distribution in cold-formed material with genetic programming," *International Journal of Advanced Manufacturing Technology*, vol. 23, no. 7-8, pp. 467–474, 2004.

[24] M. Yunus and M. S. Alsoufi, "Mathematical modelling of a friction stir welding process to predict the joint strength of two dissimilar aluminium alloys using experimental data and genetic programming," *Modelling and Simulation in Engineering*, vol. 18, pp. 1–18, 2018.

[25] A. S. Kuar, B. Acherjee, D. Ganguly, and S. Mitra, "Optimization of Nd:YAG laser parameters for microdrilling of alumina with MultiqualityCharacteristics via grey–taguchi method," *Materials and Manufacturing Processes*, vol. 27, no. 3, pp. 329–336, 2012.